


Design and control of a diagnosis and treatment aimed robotic platform for wrist and forearm rehabilitation: DIAGNOBOT

Advances in Mechanical Engineering
2018, Vol. 10(1) 1–13
© The Author(s) 2018
DOI: 10.1177/1687814017749705
journals.sagepub.com/home/ade


Mehmet Emin Aktan^{1,2} and Erhan Akdoğan¹

Abstract

Therapeutic exercises play an important role in physical therapy and rehabilitation. The use of robots has been increasing day by day in the practice of therapeutic exercises. This study aims to design and control a novel robotic platform named DIAGNOBOT for diagnosis and treatment (therapeutic exercise). It has three 1-degree-of-freedom robotic manipulators and a single grasping force measurement unit. It is able to perform flexion–extension and ulnar–radial deviation movements for the wrist and pronation–supination movement for the forearm. The platform has a modular and compact structure and is capable of treating two patients concurrently. In order to control the DIAGNOBOT, an impedance control–based controller was developed for force control, which was required for the exercises, as well as a proportional–integral–derivative controller for position control. To model the resistive exercise, an angle-dependent impedance control method different from traditional methods has been proposed. Experiments were made on five healthy subjects and it has been demonstrated that the proposed robotic platform and its controller can perform therapeutic exercises.

Keywords

Upper limb rehabilitation robot, diagnosis and treatment, variable impedance control

Date received: 31 July 2017; accepted: 23 November 2017

Handling Editor: Tadeusz Mikołajczyk

Introduction

Rehabilitation is a treatment process aimed at helping people with physical or anatomical disabilities. These disabilities might be congenital or may have occurred due to an accident, injury, or illness, and this treatment process aims to help such people achieve the highest possible level of functionality in the medical, vocational, and social spheres. Rehabilitation allows disabled people to participate in life at the highest possible level.¹ Due to the increasing world population, the need for rehabilitation is also increasing. Individuals with several limbs injured due to age, war, traffic or work-related accidents, or chronic diseases need rehabilitation to achieve full or partial recovery. A wide range of medical methods and treatments have been developed

to refunctionalize these limbs, improve their range of motion (ROM) and muscle strength. Therapeutic exercises, one of these methods, play a crucial role in the process of restoring refunctionality for disabled limbs. Therapeutic exercises have two types: passive and

¹Department of Mechatronics Engineering, Faculty of Mechanical Engineering, Yıldız Technical University, Istanbul, Turkey

²Department of Mechatronics Engineering, Faculty of Engineering, Bartın University, Bartın, Turkey

Corresponding author:

Mehmet Emin Aktan, Department of Mechatronics Engineering, Faculty of Mechanical Engineering, Yıldız Technical University, Istanbul 34349, Turkey.

Email: meaktan@yildiz.edu.tr; m.emin.aktan@gmail.com



active. These exercises can be performed by a physiotherapist or the patient himself.

There are several difficulties and limitations involved in the rehabilitation process, such as an inadequate number of doctors and physiotherapists per patient in highly populated countries, the difficulties suffered by bedridden and aged patients in reaching hospitals, the cost of the rehabilitation process, the duration of the treatment, and keeping a log and following up on the treatment process. According to a report by the Turkish Ministry of Health, the number of physiotherapists per 100.000 people in Turkey is four.² The highest number of physiotherapists is in Finland, with 202 physiotherapists per 100.000 people. Because of these reasons, the number of studies on rehabilitation robotics has seen an increase over the last two decades.³

Upper limb rehabilitation robots can be classified in terms of mechanical structure, movement capacity, variety of exercises, and control methods. The existed systems can perform one or some of the following exercises: the passive, the resistive, and the active assistive. The control methods commonly used in robotic rehabilitation are as follows: conventional control approaches, such as proportional-derivative (PD) or proportional-integral-derivative (PID), torque control, admittance control, and impedance control.

The MIT-MANUS is a well-known robotic system used for upper limb rehabilitation.⁴ The system has 3 degrees of freedom (DOFs) and can perform the passive, the active assistive, and the resistive exercises. The control method of the system is impedance control. Reinkensmeyer et al.⁵ designed a 4-DOF robot, named Assisted Rehabilitation and Measurement Guide (ARM-Guide), for the rehabilitation of the shoulder and the elbow. PD position control and torque control methods were used in the system. The REHAROB was designed using a 6-DOF industrial robot.⁶ The robot can perform passive exercises for decreasing the spasticity in the shoulder, the elbow, and the forearm. In their study, Fraile et al.⁷ designed a 2-DOF planar robotic platform, called E2Rebot, for upper limb rehabilitation in patients with neuromotor disability caused by a stroke. Besides these studies, there are many other examples of rehabilitation robots.⁸⁻¹³

A 6-DOF exoskeleton robot was developed by Nef and Riener¹⁴ for the rehabilitation of the elbow and the shoulder. The robot can perform passive- and active-assisted exercises. The control method of the system is admittance and impedance control. The use of such exoskeleton robots in rehabilitation is becoming more and more commonplace, and there are a big number of studies cited in the literature.¹⁵⁻²⁹

As seen in the literature, many robots have been developed for the rehabilitation. These robots have some limitations. These limitations are DOF, independence of operating of axes, grasping of end-effector

(handle), and inability for diagnosis. First, robotic manipulators have one or more DOFs in a single structure. This leads to limitations both in the control of the system and in the force and torque measurements to be made for each axis for diagnosis. Second, the failure of one of the axis also affects other axes. These robots allow for the treatment of only one patient at the same time. Third, in the previous designs, the patients grasp the end-effector. This way is not effective in stroke patients who cannot grasp. Finally, existed designs are not suitable for diagnosis.

To overcome these limitations, a novel robotic platform has been developed in this study. The developed system called DIAGNOBOT consists of three 1-DOF robotic manipulators and a single grasping force measurement unit. The most important feature of this system is that it can perform diagnosis and treatment simultaneously. For this purpose, it is equipped with sensors and actuators developed in a suitable mechanical structure. The force and torque sensors are located in the direction of movement. The robot manipulators for each movement were placed on a rotating table. Each unit can easily be removed and installed. It ensures that the robotic system is modular and configurable. Because the units are independent of each other, it allows for the treatment of two patients at the same time. Thanks to this design, the failure of a unit does not affect other units. The robot manipulators are designed according to stroke patients and they do not need to grasp manipulators (handles). The developed system can perform flexion-extension and ulnar-radial deviation movements for the wrist, and pronation-supination movement for the forearm. It can perform the passive, isometric, isotonic, and resistive therapeutic exercises. DIAGNOBOT controller has a force-based impedance control structure for the isotonic exercise. For variable resistive exercises, a novel impedance-based control method has been developed. In this method, the force on the end-effector changes depends on the joint angle. Therefore, this new control approximation is called the *angle-dependent impedance control*. This method's efficiency has been confirmed through experiments made with five healthy subjects. On the other hand, PID control was used for the passive exercise.

There are two contributions to the literature in this study. The former is the unique design of the robotic platform both diagnosis and treatment for upper limb rehabilitation, the latter is the development of a controller based on angle-dependent impedance control to model resistive exercises. An explanatory video about the developed system can be reached in the link.³⁰

This article is organized as follows: the theory of upper limb rehabilitation is specified first, followed by the mechanical design, electronics hardware, strength and limitations, the dynamics, and the control and operation, respectively. Finally, the results and the conclusion are given.

Theory of upper limb rehabilitation

Therapeutic exercises are performed to improve the strength, endurance, coordination, speed, and skills of the limbs. They can be passive or active and can be performed manually or by an assistive device. Therapeutic exercises are considered as one of the important stages of the physical therapy and rehabilitation. In this study, the therapeutic exercises are performed for the rehabilitation of the wrist and the forearm.

Movements of limbs

The developed rehabilitation robot can perform flexion–extension and ulnar–radial deviation movements for the wrist, and pronation–supination movements for the forearm. The definitions of these movements are given in Figure 1 and explained below.

Flexion–extension. Bending the wrist upward is called the extension and downward the flexion movement. The wrist is initially parallel to the ground and the palm faces downward.

Ulnar–radial deviation. Bending the wrist upward is called the radial deviation and downward the ulnar deviation movement. The palm faces sideways with the thumb in natural position.

Supination–pronation. Supination is the rotation of the forearm so that the wrist faces up. When it faces downward, it is called the pronation movement.

Types of therapeutic exercises

The rehabilitation robot developed in this study can perform the passive, isometric, isotonic, and resistive therapeutic exercises for the upper limb. The definitions of these exercises are given below.

Passive exercise. The passive exercise is performed manually or by assistive device within the motion range of

the limb. It does not include the coordinated voluntary muscle contraction of the patient.

Isometric exercise. Through this exercise, the level of muscle contraction is increased without causing a change in the length of the muscle. It can be performed by pressing a stationary object, opposing the manual act of the physiotherapist, or by holding a weight in a static condition.

Isotonic exercise. In the isotonic exercise, the limb is moved along the ROM against a constant force. Additionally, an exercise mode, in which the various difficulty levels are determined by the impedance control parameters, was created in this study. This mode is called the *vario-resistive exercise* mode.

Design of DIAGNOBOT

This section highlights design aspects, including functional requirements and design parameters, the mechanical structure, the electronics hardware, and strength and limitations of the DIAGNOBOT.

Functional requirements and design parameters

The functional requirements of the DIAGNOBOT are as follows:

1. Perform the movements of flexion–extension, ulnar–radial deviation, and pronation–supination for the wrist and the forearm.
2. Measure the grasping force of the hand and angle of wrist and forearm for diagnosis.
3. Perform the passive, isotonic, isometric, and vario-resistive therapeutic exercises.
4. Treat two patients at the same time.
5. Make it possible to fix the wrist in the pronation–supination movement.
6. Adjust the length of each manipulator according to the size of the limb.
7. Provide safety via software and hardware.

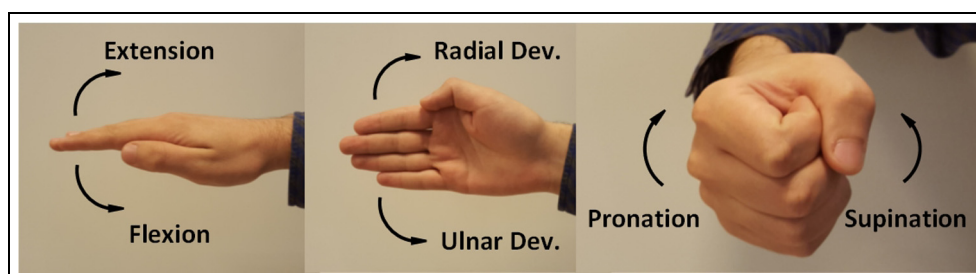


Figure 1. The movements of the wrist and the forearm.

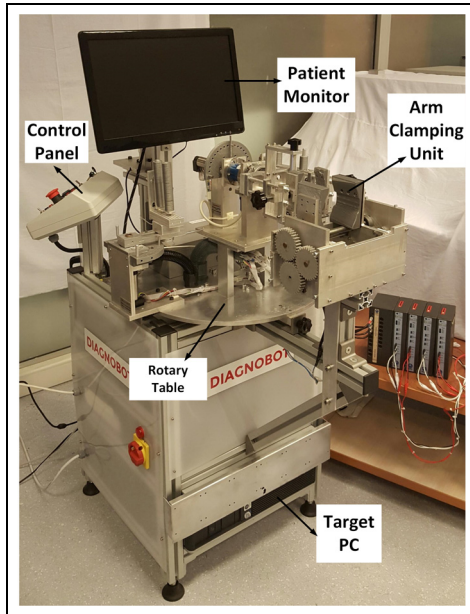


Figure 2. The general structure of DIAGNOBOT.

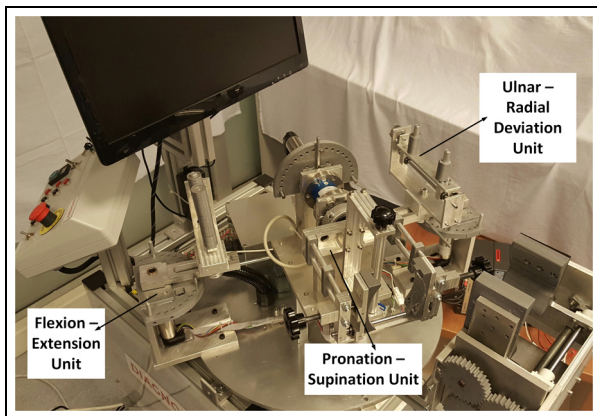


Figure 3. The units of DIAGNOBOT.

The design parameters that meet the functional requirements are as follows:

1. There are three 1-DOF robot manipulators for each movement.
2. There is a grasping force measurement unit.
3. There are three servo motors for the therapeutic exercises required force and position control.
4. The robot manipulators are placed on the rotary table that allows simultaneous use.
5. There are two clamping screws on the pronation-supination unit.
6. Each manipulator can be adjusted with screws and pins in accordance with the size of the limb.
7. The system has three safety layers in terms of mechanical, electronics, and software.

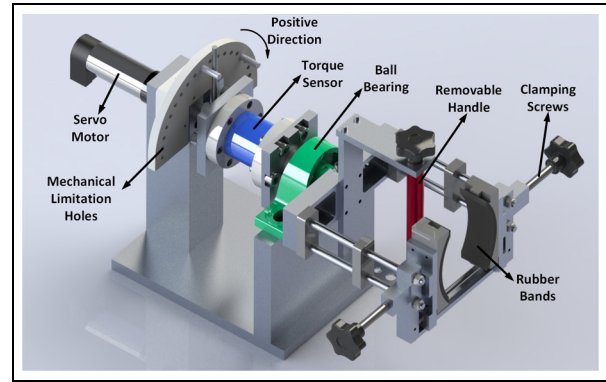


Figure 4. The structure of the pronation-supination unit.

Mechanical structure

The general structure of the DIAGNOBOT and its units are shown in Figures 2 and 3. The arm of the patient is placed in the arm clamping unit and fastened between the jaws actuated by the stepper motor. All units are placed on the rotary table. According to the type of movement, the relevant unit turns in front of the patient. The rotary table and the stepper motor that actuates the arm clamping unit are controlled by the buttons on the control panel. There is an emergency button on this panel. In front of the patient, there is a patient monitor, showing the games and directions of the exercises. There are mechanical limitation holes and pins at each unit for safety. The ROM of the manipulator can be adjusted for any patient and exercise by inserting the pins into the holes. For all manipulators, the clockwise is the positive direction and the counter-clockwise is the negative direction. The details about the units are given below.

The pronation-supination unit is shown in Figure 4. This unit performs the movement of pronation-supination for the forearm. It contains a servo motor for actuation and a torque sensor for the measurement of the joint torque. The patient can be fixed to this unit in two ways. The first is, the patient grasps the removable handle with his or her hand. This is not possible in stroke patients and patients who cannot grasp. The second way is fixing of the patient's wrist. In this way, the handle is removed. The patient's wrist is fixed between the jaws of the unit through the clamping screws. There are rubber pads on these jaws to avoid causing any pain. In the pronation-supination movement, the arm is not fixed by the arm clamping unit. The two types of the fastening can be seen in Figure 5.

The flexion-extension and ulnar-radial deviation units are shown in Figure 6. These units perform movements of the wrist. Each unit contains a servo motor for actuation and a force sensor for the measurement of the joint force. The patient's hand is placed between the bars of the handle. In the flexion-extension and

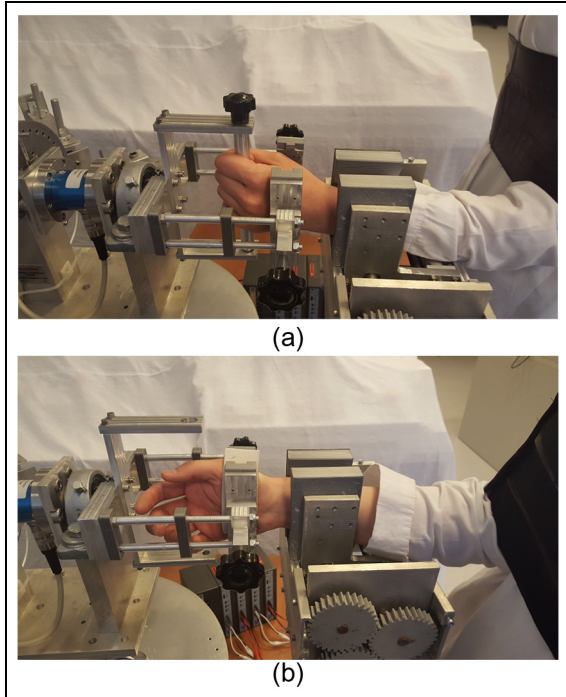


Figure 5. The fixing to the pronation–supination unit: (a) grasping the removable handle and (b) fixing the wrist of patient.

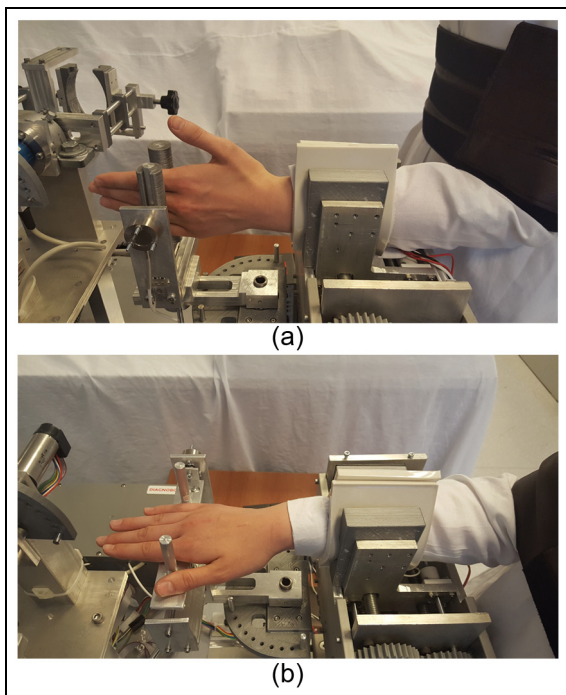


Figure 6. The flexion–extension and ulnar–radial deviation units: (a) the movement of the flexion–extension and (b) the movement of the ulnar–radial deviation.

ulnar–radial deviation movements, the patient's arm has to be fixed with the arm clamping unit.

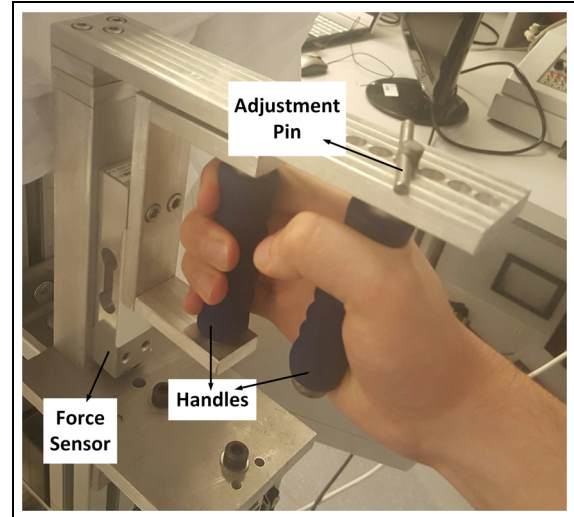


Figure 7. The grasping force measurement unit.

The grasping force measurement unit can be seen in Figure 7. The grasping force is the major measurement for the diagnosis. This unit measures the grasping force of the patient. The unit contains a force sensor to measure the grasping force.

Electronics hardware

The block diagram of the electronics hardware is shown in Figure 8. The doctor is the main user of the system. He enters all the information relevant to the therapy. There are three computers in the system: the Main PC for running the algorithms, the Target PC for real-time operations, and the Raspberry Pi for games of isometric, isotonic, and vario-resistive exercises. The algorithms were developed in MATLAB R2017a. The Simulink[®] Real Time is used for the real-time prototyping. The TCP/IP protocol is used for the communication between the Main PC and the Target PC. The communication between the Main PC and the Raspberry Pi is provided by UDP Protocol.

There are three servo motors (Maxon EC-Max 30) with the 103:1 reduction ratio and 500 pulse/rev encoders. There are also three servo motor drivers (Maxon EPOS 2 50/5) in the system.

There are three force sensors and a torque sensor in the system. Two Burster 8523-200 force sensors are used to measure the patient force in the flexion–extension and ulnar–radial deviation units. The Burster 8627-5710 torque sensor is used in the pronation–supination unit. The Loadstar RSP1-050M force sensor is used to measure the grasping force. The measurement ranges of each sensor are given in Table 1.

In the system, for the encoder input and analog input/output data, Measurement Computing PCI

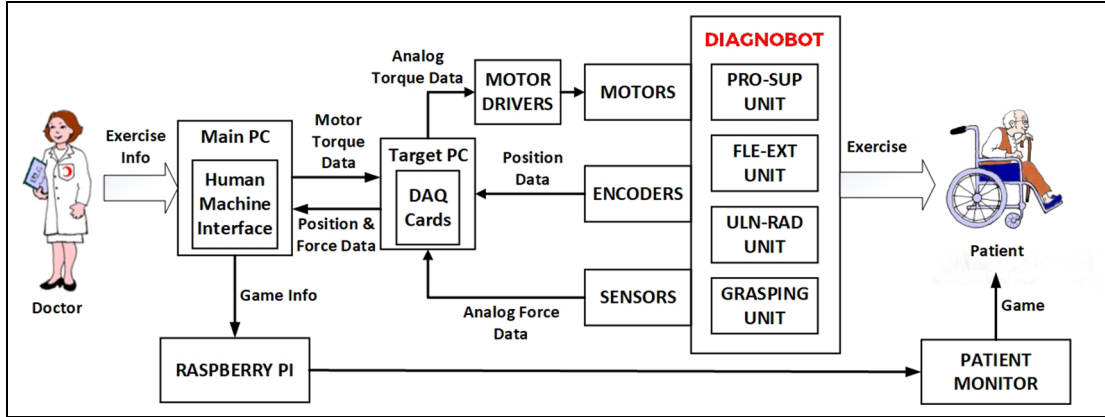


Figure 8. The block diagram of the electronics hardware.

Table 1. The measurement ranges of the sensors.

Sensors	Range
Torque sensor	$\pm 10 \text{ N m}$
Force sensors for units	$\pm 200 \text{ N}$
Force sensor for grasping unit	50 kg

QUAD04, NI PCI-6024E, and NI PCI-6040E data acquisition cards are used with 1-ms sampling time, respectively.

Safety is extremely important for robots that interact with humans. Therefore, various mechanical, electrical, and software-based safety measures are integrated into the developed system. They are given as follows:

1. Each manipulator's ROM is in line with the ROM of the joints.
2. Each servo motor has current limitation.
3. There is a current leakage relay.
4. There are two emergency stop buttons for the patient and the doctor.
5. The high-voltage (220 V) connections are located in the insulated enclosure.
6. Each manipulator has software-based limitations.

Strengths and limitations

The developed robotic platform has a number of strengths and limitations. It has a modular structure thanks to the exchangeable units. The failure of a unit does not affect the other units. This is very convenient for force/torque and ROM measurements for diagnostics. It provides home-based robotic rehabilitation for bedridden and elderly patients. On the other hand, there are limitations such as the lack of motivation and

confidence for patients who are accustomed to traditional methods.

Dynamics of DIAGNOBOT

Obtaining the mathematical model of the robot manipulator is very important for the control. The dynamic parameters must be calculated correctly to achieve a good control performance in the impedance control method. In this section, dynamic equations are obtained and the dynamic parameters of the system are calculated using the experimental robot identification through the optimized periodic trajectories method.³¹

The single-link robot manipulator's dynamic equation is shown in the following equation

$$\tau = M\ddot{q} + gm_r \sin(q) + gm_x \cos(q) + f_v(\dot{q}) + f_c \text{sign}(\dot{q}) \quad (1)$$

where M is the total inertia of the link, motor, and the gear. The g is the gravity force. The q , \dot{q} , and \ddot{q} are the angular position, the velocity, and the acceleration of the robot joint, respectively. The m is the mass of the link. The r_y and r_x are the y and x positions of the center of the mass, respectively. The f_v and f_c are the viscous and Coulomb friction coefficients, respectively.

System identification and parameter estimation

The inverse dynamics of equation (1) can be expressed by following equation

$$\tau = [\ddot{q} \quad g \cdot \sin(q) \quad g \cdot \cos(q) \quad \dot{q} \quad \text{sign}(\dot{q})] \cdot \begin{bmatrix} M \\ mr_y \\ mr_x \\ f_v \\ f_c \end{bmatrix} = \phi(q, \dot{q}, \ddot{q}) \cdot p \quad (2)$$

In this equation, the robot position, velocity, and acceleration are the known parameters. The vector p consists of unknown parameters. If a minimum of six different vector ϕ and τ values corresponding to vector ϕ is known, vector p can be calculated. This is called the *parameter estimation method*.

However, there are errors in the measurement of the speed and the acceleration of the link and the robot torque. For this reason, more than six different points are used and it is ensured that the robot manipulator follows a predetermined trajectory through a PID controller. Consider we have observations data ($i \in 1, \dots, M$), we can solve the equation of

$$Y = W \cdot p \quad (3)$$

$$W = \begin{bmatrix} \phi(q^1, \dot{q}^1, \ddot{q}^1) \\ \phi(q^2, \dot{q}^2, \ddot{q}^2) \\ \vdots \\ \phi(q^M, \dot{q}^M, \ddot{q}^M) \end{bmatrix} \quad Y = \begin{bmatrix} \tau^1 \\ \tau^2 \\ \vdots \\ \tau^M \end{bmatrix} \quad (4)$$

The condition number of the matrix W represents how close the solution to the nonlinear differential equation is. In order to obtain the optimal trajectory, the optimal solution is found which makes the condition number of the matrix W minimum. The *fmincon* function of the MATLAB was used for the solution. Let us represent the trajectories as a finite Fourier series

$$q(t) = \sum_{l=1}^N \frac{a_l}{\omega_f l} \sin(\omega_f l t) - \frac{b_l}{\omega_f l} \cos(\omega_f l t) + q_0 \quad (5)$$

$$\dot{q}(t) = \sum_{l=1}^N a_l \cos(\omega_f l t) + b_l \sin(\omega_f l t) \quad (6)$$

$$\ddot{q}(t) = \sum_{l=1}^N -a_l \omega_f l \sin(\omega_f l t) + b_l \omega_f l \cos(\omega_f l t) \quad (7)$$

where ω_f is the fundamental pulsation of the Fourier series, a_l and b_l are the coefficients, N is the number of harmonics, and q_0 is the robot configuration around which the robot excitation occurs. Boundary conditions for position, velocity, and acceleration can be given while obtaining the optimal trajectory. These boundary conditions are shown as follows

$$\begin{aligned} \delta^* &= \arg \min \text{cond}(\delta, \omega_f) \\ q_{\min} &\leq q(t) \leq q_{\max} \\ -q_{\max} &\leq \dot{q}(t) \leq \dot{q}_{\max} \\ -\ddot{q}_{\max} &\leq \ddot{q}(t) \leq \ddot{q}_{\max} \end{aligned} \quad (8)$$

where δ is the vector containing Fourier coefficients. δ^* is the optimal δ which minimizes the condition number of matrix W . In the optimization, $\omega_f = 0.1$, $N = 5$, $q_{\min} = -90^\circ$, and $q_{\max} = 90^\circ$ were selected. The

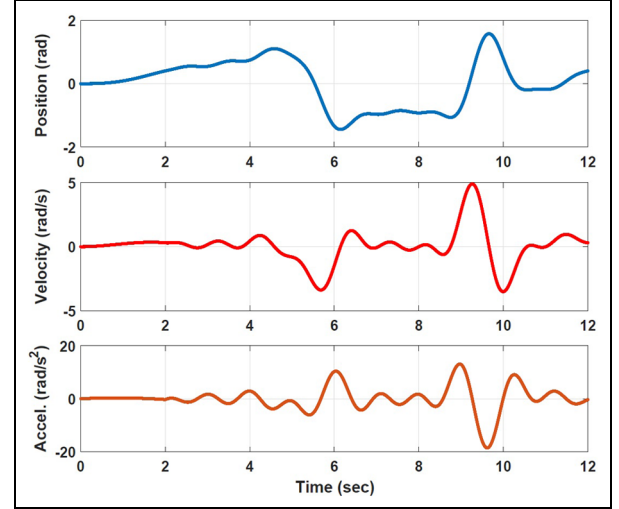


Figure 9. The optimal trajectory.

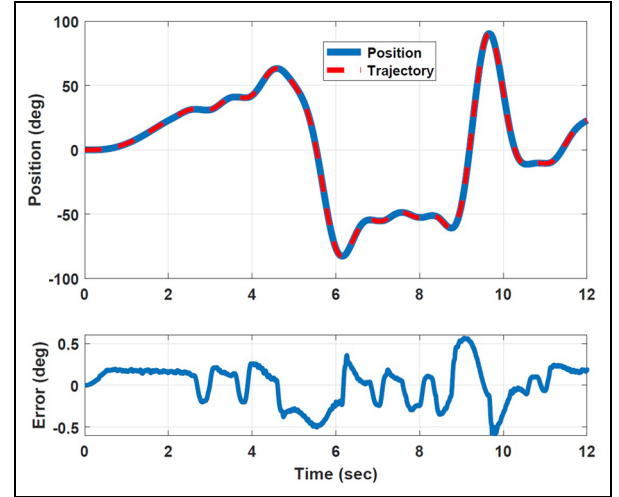


Figure 10. The optimal trajectory, position of manipulator, and error.

optimal trajectory obtained is shown in Figure 9. With a PID controller, the robot manipulator for each unit is followed to this trajectory and the q , \dot{q} , \ddot{q} values are saved and vector W is obtained. The position of the robot manipulator, optimal trajectory, and the error in the pronation–supination unit can be seen in Figure 10. The torque values applied by the servo motor during the following of the optimal trajectory are also saved and the Y vector is obtained. The dynamic parameters of the system are identified using the least square estimation method below

$$p = (W^T W)^{-1} W^T Y \quad (9)$$

The obtained dynamic parameters are given in Table 2.

Table 2. Estimated parameters for each manipulator.

Parameters	Pro-Sup	Fle-Ext	Uln-Rad	
M	0.0277	0.0091	0.0177	kg m ²
mg_{\cos}	0.0082	0.0025	0.0018	kg m
mg_{\sin}	0.0182	0.0048	0.0027	kg m
f_v	0.0733	0.0243	0.0374	N ms/rad
f_c	0.1333	0.0766	0.0821	N m

Control and operation of DIAGNOBOT

The basis of the robotic rehabilitation is the human-machine interaction. The impedance control method developed by Hogan is the most suitable control method for this interaction.^{32,33} The impedance control method can perform based on position and force control. Therapeutic exercises require force and position control. The PID control, force-based impedance control, and angle-dependent impedance control, which is proposed in this study, are used in the developed robotic platform.

Angle-dependent impedance control

The dynamic behavior of the robot manipulator after applying force-based impedance control can be explained as follows

$$M_d \ddot{x} + B_d \dot{x} - F_d = -F_e \quad (10)$$

where M_d and B_d are 2×2 diagonal matrices that denote the desired inertia and damping. The 2×1 vectors F_d and F_e are the desired force and force measured by the sensor, respectively. Equation (10) is formulated as

$$\ddot{x} = M_d^{-1}(-B_d \dot{x} + F_d - F_e) \quad (11)$$

where x denotes the position of the end-effector. The velocity and acceleration is

$$\dot{x} = J(q)\dot{q} \quad (12)$$

$$\ddot{x} = J(q)\ddot{q} + \dot{J}(q)\dot{q} \quad (13)$$

Equation (13) yields this result

$$\ddot{q} = J(q)^{\dagger}(\ddot{x} - \dot{J}(q)\dot{q}) \quad (14)$$

where $J(q)^{\dagger}$ denotes the pseudoinverse of the 2×1 Jacobian vector $J(q)$. This formula is replaced by equation (1) to obtain the general torque equation

$$\tau = MJ(q)^{\dagger}(M_d^{-1}(F_d - F_e - B_d \dot{x}) - \dot{J}(q)\dot{q}) + gm_{r_y} \sin(q) + gm_{r_x} \cos(q) + f_v(\dot{q}) + f_c \text{sign}(\dot{q}) + J(q)^T F_e \quad (15)$$

The relationship between the joint angle and the joint force/torque was examined in the experiments with 10 healthy subjects. The results for the pronation-supination are shown in Figure 11.

As a result of the experiments, it is seen that there is an inverse relationship between the joint torque and the joint angle. As the ROM increases, the torque produced by the joint decreases. This result should be taken into consideration in order to improve the performance of the resistive exercises. B_d is the constant in equation (15). In the angle-dependent impedance control method, B_d changes depending on the angle of the joint. B_d is the maximum when the joint angle is at 0° ($B_{d_{\max}}$). As the joint moves toward the maximum ROM,

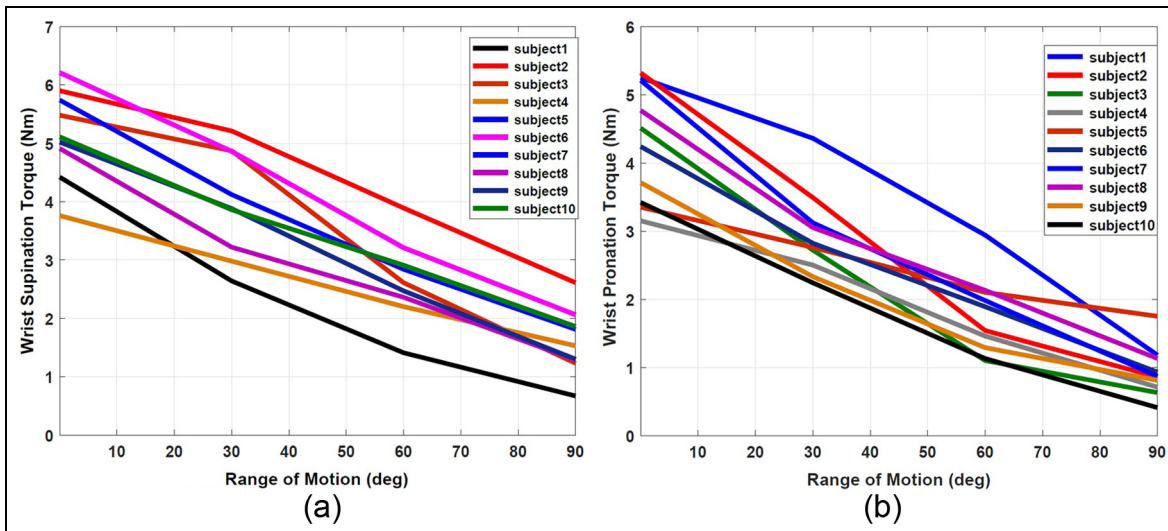


Figure 11. The wrist torques depending on the joint angles: (a) the relationship between the supination torque and ROM and (b) the relationship between the pronation torque and ROM.

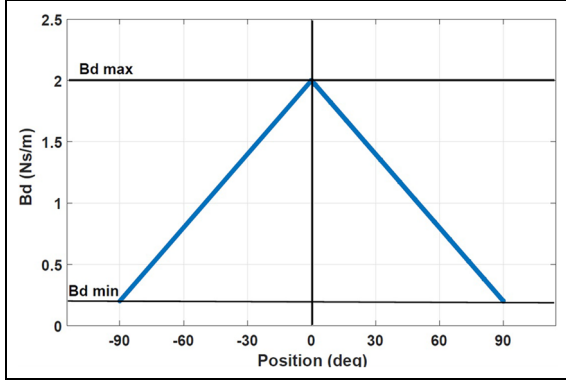


Figure 12. The relationship between position and B_d .

the B_d decreases and when the maximum ROM is reached, the B_d gets the smallest value ($B_{d_{min}}$)

$$\Delta B_d = B_{d_{max}} - B_{d_{min}} \quad (16)$$

The change of B_d can be written depending on the actual position (θ) and maximum position (θ_{max})

$$B_d = \Delta B_d \frac{(\theta_{max} - |\theta|)}{\theta_{max}} \quad (17)$$

When θ reaches the θ_{max} value, B_d becomes zero. This leads to the instability of the system. For this reason, the ($B_{d_{min}}$) is added to equation (17) and the following equation is obtained

$$B_d = [(\theta_{max} - |\theta|)(B_{d_{max}} - B_{d_{min}})(\theta_{max}^{-1})] + B_{d_{min}} \quad (18)$$

When the $\theta_{max} = 90^\circ$, $B_{d_{max}} = 2 \text{ N s/m}$, and $B_{d_{min}} = 0.2 \text{ N s/m}$, the position– B_d plot can be seen in Figure 12.

The resulting control law after combining equations (15) and (18) becomes

$$\begin{aligned} \tau = & MJ(q)^\dagger (M_d^{-1} (F_d - F_e - [(\theta_{max} - |\theta|) \\ & (B_{d_{max}} - B_{d_{min}})(\theta_{max}^{-1})] + B_{d_{min}} \dot{x}) - \dot{J}(q)\dot{q}) + gmr_y \sin(q) \\ & + gmr_x \cos(q) + f_v(\dot{q}) + f_c \text{sign}(\dot{q}) + J(q)^T F_e \end{aligned} \quad (19)$$

PID control

The PID algorithm is described by

$$u(t) = K_p e(t) + K_i \int_0^t e(t) dt + K_d \dot{e}(t) \quad (20)$$

where K_p , K_i , and K_d are the constants of the proportional, integral, and derivative, respectively.

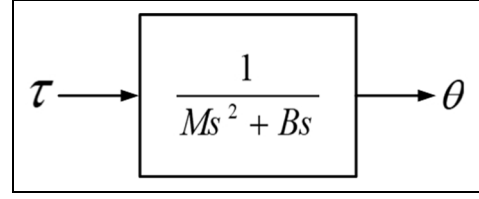


Figure 13. The transfer function block of the inertia–damper system.

Verification of dynamic parameters

The M_d and B_d in equation (15) express the inertia and damping felt in the end-effector of the robot manipulator. The achievement of this sensation with high precision depends on the accuracy of the robot dynamic parameters. A simulation was performed to test the accuracy of the dynamic parameters in equation (1). The simulation results are compared with the values obtained from the system. A system consisting of inertia (M) and damping (B) with torque τ as input and position (θ) as output is shown in Figure 13.

A control model was created using MATLAB Simulink according to equation (15) and the torque manually applied to the end-effector of the robot manipulator. The M_d and B_d values are entered as 0.03 kg m^2 and 0.3 N m/s , respectively. The applied torque and position trajectory are recorded. Then, the recorded torque value is used as an input of the transfer function shown in Figure 13 and simulated. The M and B values in the transfer function were selected the same as in the experiment (0.03 kg m^2 and 0.3 N m/s). The position values obtained from experiment θ_{exp} and simulation θ_{sim} are compared and shown in Figure 14.

According to the simulation results, the position error between the experiment and simulation is smaller than 10° in supination and 5° in pronation. It shows that the inertia and damping values set in the equation and felt in the end-effector of the robot are close to each other. These results show that the system dynamic parameters are estimated correctly.

Human–machine interface

The HMI provides the communication between the doctor, the patient, and the DIAGNOBOT. The HMI consists of the main controller, the graphical user interface (GUI), the PID controller, and the impedance controller. The main controller is responsible for the communication between all of the units. The doctor enters the exercise information and parameters through the GUI. According to the exercise information, exercise parameters are sent to the PID or impedance controller. In addition, the trajectory and target force information for a certain type of exercise is also sent to

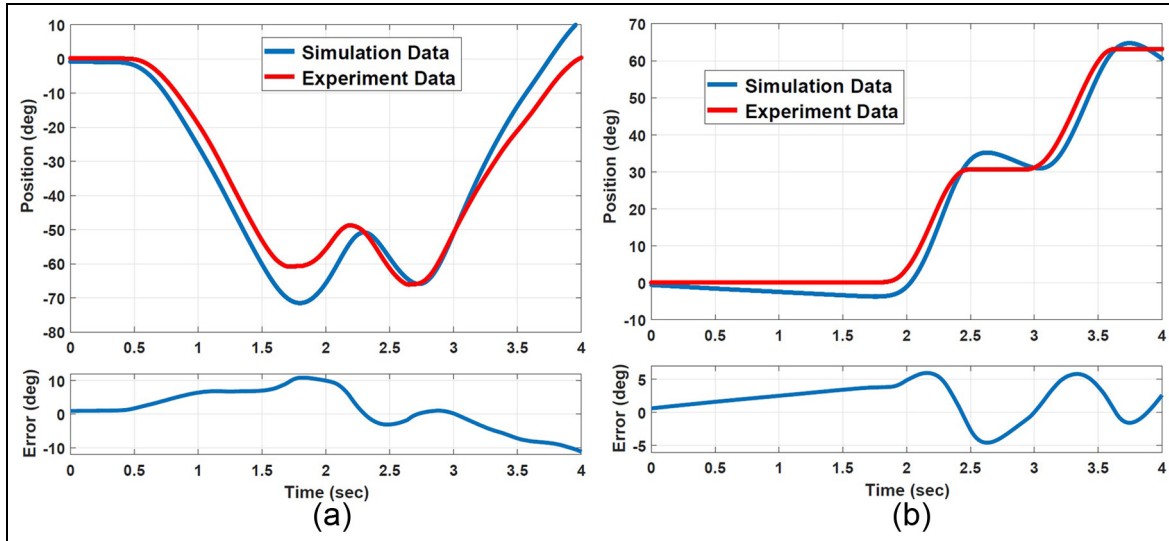


Figure 14. The comparison of the experiments and the simulation results: (a) experiment and simulation result in supination and (b) experiment and simulation result in pronation.

Table 3. Physical properties of the subjects.

Subject	Age	Weight (kg)	Height (cm)	Sex
A	29	73	175	Male
B	27	67	175	Male
C	28	84	186	Male
D	31	80	177	Male
E	26	77	179	Male

the related controller. At the end of each exercise, the information about the session, such as the type of the exercise, the ROM, the force/torque values, the grasping force measurements before and after the treatment, and the performance evaluation of the exercise, is recorded in the database.

The passive, isotonic, and isometric exercises are performed by the HMI interface. In addition to these conventional exercise types, a novel exercise mode, named vario-resistive exercise, was developed in this study. Detailed explanations as to the exercise types are given in the next section.

Evaluation and results

The performance of the system is tested by voluntary subjects. The tests were performed under the supervision of a doctor. The passive, isotonic, and vario-resistive exercises were performed by five healthy subjects. The physical properties of the subjects are given in Table 3. The input data according to the type of exercise were entered by the doctor via GUI. All

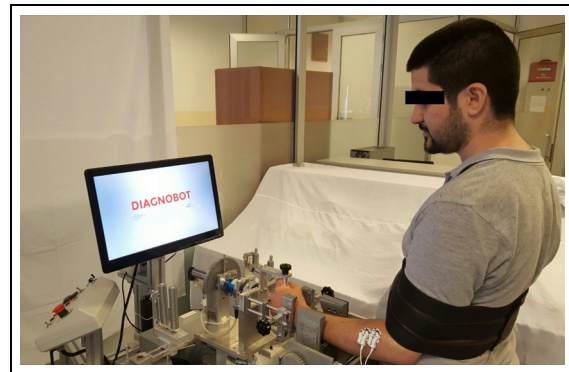


Figure 15. An experiment with a healthy subject.

movements were repeated five times. A snapshot of an experiment with a healthy subject is given in Figure 15. The results of the experiments are presented in the following subsections.

Passive exercise

In the passive exercise, the robot manipulator moves the patient's limb within the ROM defined by the doctor. The position trajectory is generated by HMI according to the information entered on the speed and the motion limits. The doctor also enters the type of movement and the number of repetition from the GUI. This exercise requires position control, and the controller is in the PID control mode. An example of graphical results can be seen in Figure 16. According to the results of the experiments, the robot manipulator was

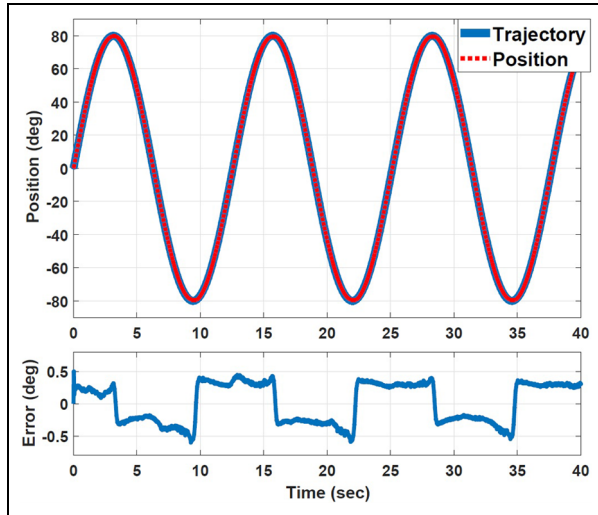


Figure 16. Passive flexion–extension exercise result for subject A.

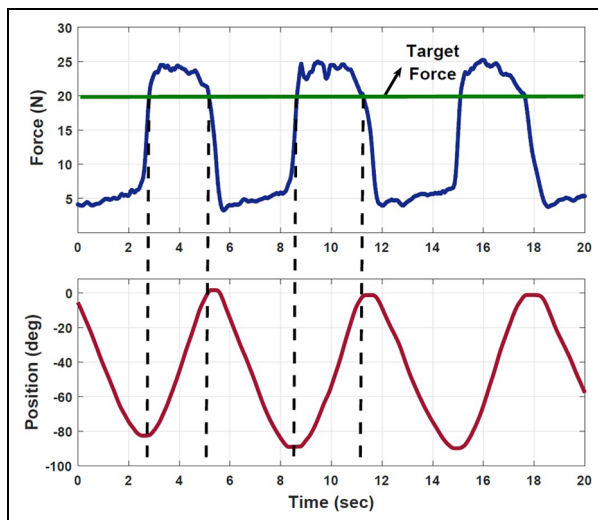


Figure 17. The isotonic flexion–extension exercise result for subject B.

able to track the desired trajectory with a margin of error below 0.5° .

Isotonic exercise

In the isotonic exercise, the subject moves his limb against an opposing force generated by the robot manipulator. The robot manipulator resisted to the motion of the subject by applying the opposite force defined by the doctor. When the patient exceeds this target force value, the robot starts moving. If the limb force drops below this target force value, the robot forces the joint to move in the opposite direction. The controller is in the force-based impedance control

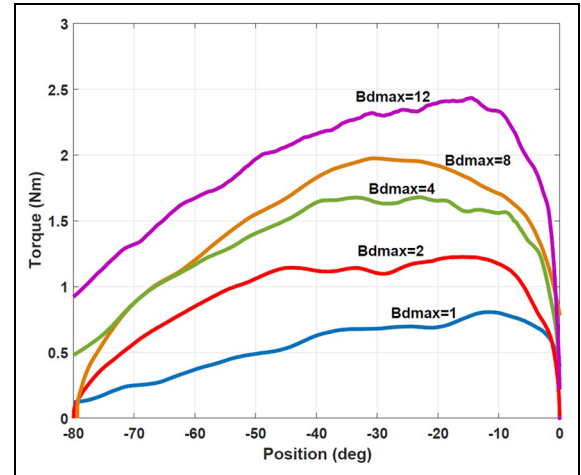


Figure 18. The vario-resistive therapy results at different $B_{d_{max}}$ in pronation.

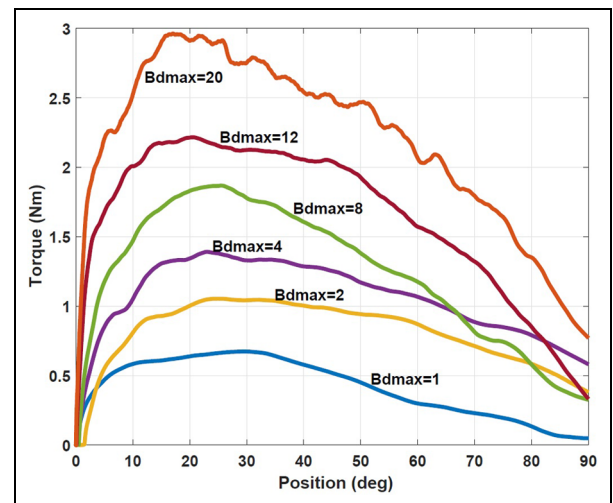


Figure 19. The vario-resistive therapy results at different $B_{d_{max}}$ in supination.

mode. An example of graphical results can be seen in Figure 17. It is understood that the robot manipulator can perform the isotonic exercises.

Vario-resistive exercise

This exercise differs from traditional resistive exercises. In our proposed mode, the resistance changes depending on the joint angle. Thus, the patient does not have difficulty increasing the joint angle and can perform the exercise highly successfully. The controller is in the angle-dependent impedance control mode. The results of the vario-resistive exercise for pronation–supination can be seen in Figures 18 and 19. The exercises were

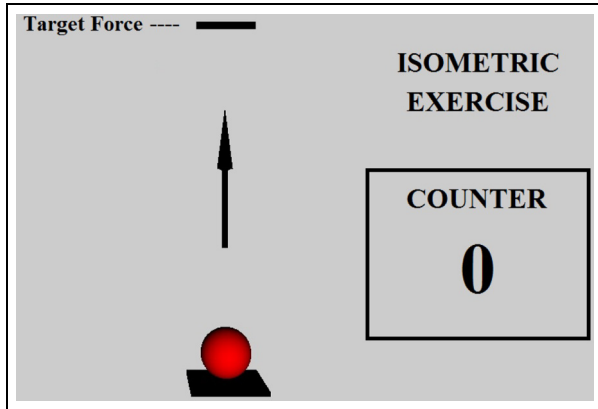


Figure 20. The game screen of the isometric exercise.

performed with different damping (B_d) values. The torque applied by the patient to the manipulator during exercise was measured with the torque sensor. As seen in the figures, as the ROM value increases, the torque value required to perform the motion decreases. This shows that vario-resistive exercise mode operates accurately.

Isometric exercise

In this type of exercise, the patient tries to reach the target force while the end-effector is stationary. The doctor enters the type of movement, the target force/torque, and the starting position. At the beginning of the exercise, the robot manipulator moves to the starting position. In this position, the patient applies a force to the manipulator. The patient follows his or her force value and target force value from the game screen. In the developed game, the patient tries to reach the target position with the ball moving according to the limb force. This exercise requires position control to move the target position. Because of that, the PID controller was used. The game screen is shown in Figure 20.

Conclusion

In this study, a novel robotic platform named DIAGNOBOT was designed and controlled to perform diagnosis and treatment in wrist and forearm rehabilitation. An impedance controller and PID-based controller were developed to control the DIAGNOBOT. The developed controller consists of an angle-dependent impedance controller designed for modeling resistive exercises that differ from traditional methods normally used for modeling resistive exercises. This controller was tested with five healthy subjects. Experimental results show that the developed controller can model resistive and passive exercises accurately. In order to further this study, the system will be tested with more data from healthy subjects and patients.

Furthermore, the developed intelligent diagnosis and treatment control structure will be introduced. In particular, there will be greater focus on deep learning algorithms for diagnosis.

Acknowledgement

The authors would like to thank Prof. Dr. K. Banu Kuran and Dr. Ahmet Taha Kuru for their valuable contributions.

Declaration of conflicting interests

The author(s) declared no potential conflicts of interest with respect to the research, authorship, and/or publication of this article.

Funding

The author(s) disclosed receipt of the following financial support for the research, authorship, and/or publication of this article: This work was supported by Research Fund of the Yildiz Technical University (project number: 2015-06-04-DOP01).

References

1. Akdemir N and Akkuş Y. Rehabilitasyon ve hemşirelik (derleme). *Hemşire Yüksek Derg* 2006; 13: 82–91.
2. Küçük A, Süleklı H and Mortaş A. *OECD, Avrupa Birliđi Sađlık İstatistikleri Ve Türkiye*. Statistical report, 2015, <http://www.saglikaktuel.com/d/file/35c966a9f1d343909d4d0858bec69333.pdf>
3. Krebs HI. An overview of rehabilitation robotic technologies. In: *Proceedings of American spinal injury association symposium*, 2006.
4. Krebs HI, Hermano I, Hogan N, et al. Robot-aided neurorehabilitation. *IEEE Trans Rehabil Eng* 1998; 6: 75–87.
5. Reinkensmeyer DJ, Kahn LE, Averbuch M, et al. Understanding and treating arm movement impairment after chronic brain injury: progress with the arm guide. *J Rehabil Res Dev* 2000; 37: 653–662.
6. Toth A, Fazekas G, Arz G, et al. Passive robotic movement therapy of the spastic hemiparetic arm with REHAROB: report of the first clinical test and the follow-up system improvement. In: *Proceedings of 9th international conference on rehabilitation robotics (ICORR 2005)*, Chicago, IL, 28 June–1 July 2005, pp.127–130. New York: IEEE.
7. Fraile JC, Pérez-Turiel J, Baeyens E, et al. E2Rebot: a robotic platform for upper limb rehabilitation in patients with neuromotor disability. *Adv Mech Eng* 2016; 8: 1–13.
8. Kahn LE, Averbuch M, Rymer WZ, et al. Comparison of robot-assisted reaching to free reaching in promoting recovery from chronic stroke. In: *Proceedings of the international conference on rehabilitation robotics*, Amsterdam, 2001, pp.39–44.
9. Lum P, Reinkensmeyer D, Mahoney R, et al. Robotic devices for movement therapy after stroke: current status and challenges to clinical acceptance. *Top Stroke Rehabil* 2002; 8: 40–53.

10. Atlihan M, Akdoğan E and Arslan MS. Development of a therapeutic exercise robot for wrist and forearm rehabilitation. In: *Proceedings of 19th international conference on methods and models in automation and robotics (MMAR)*, Międzyzdroje, 2–5 September 2014. New York: IEEE.
11. Dukelow SP. Potential of robots as next-generation technology for clinical assessment of neurological disorders and upper-limb therapy. *J Rehabil Res Dev* 2011; 48: 335–353.
12. Akdoğan E, Taçgın E and Adli MA. Knee rehabilitation using an intelligent robotic system. *J Intell Manuf* 2009; 20: 195–202.
13. Akdoğan E and Adli MA. The design and control of a therapeutic exercise robot for lower limb rehabilitation: physiotherobot. *Mechatronics* 2011; 21: 509–522.
14. Nef T and Riener R. Armin—design of a novel arm rehabilitation robot. In: *Proceedings of 9th international conference on rehabilitation robotics (ICORR 2005)*, Chicago, IL, 28 June–1 July 2005, pp.57–60. New York: IEEE.
15. Sanchez JR, Wolbrecht E, Smith R, et al. A pneumatic robot for re-training arm movement after stroke: rationale and mechanical design. In: *Proceedings of 9th international conference on rehabilitation robotics (ICORR 2005)*, Chicago, IL, 28 June–1 July 2005, pp.500–504. New York: IEEE.
16. Stopforth R. Customizable rehabilitation lower limb exoskeleton system. *Int J Adv Robot Syst* 2012; 9: 152.
17. Wu Q, Wang X and Du F. Development and analysis of a gravity-balanced exoskeleton for active rehabilitation training of upper limb. *Proc IMechE, Part C: J Mechanical Engineering Science* 2016; 230: 3777–3790.
18. Denève A, Moughamir S, Afilal L, et al. Control system design of a 3-DOF upper limbs rehabilitation robot. *Comput Method Programs Biomed* 2008; 89: 202–214.
19. Kim B and Deshpande AD. An upper-body rehabilitation exoskeleton harmony with an anatomical shoulder mechanism: design, modeling, control, and performance evaluation. *Int J Robot Res* 2017; 36: 414–435.
20. Moubarak S, Pham MT, Pajdla T, et al. Design and modeling of an upper extremity exoskeleton. In: *Proceedings of world congress on medical physics and biomedical engineering*, Munich, 7–12 September 2009, pp.476–479. Berlin: Springer.
21. Kiguchi K, Kose Y and Hayashi Y. An upper-limb power-assist exoskeleton robot with task-oriented perception-assist. In: *Proceedings of 3rd IEEE RAS and EMBS international conference on biomedical robotics and biomechatronics (BioRob)*, Tokyo, Japan, 26–29 September 2010, pp.88–93. New York: IEEE.
22. Long Y, Du ZJ, Wang W, et al. Development of a wearable exoskeleton rehabilitation system based on hybrid control mode. *Int J Adv Robot Syst* 2016; 13: 6487.
23. Kiguchi K and Hayashi Y. An EMG-based control for an upper-limb power-assist exoskeleton robot. *IEEE T Syst Man Cy B* 2012; 42: 1064–1071.
24. Mao Y and Agrawal SK. Design of a cable-driven arm exoskeleton (CAREX) for neural rehabilitation. *IEEE T Robot* 2012; 28: 922–931.
25. Wei W, Guo S, Zhang W, et al. A novel VR-based upper limb rehabilitation robot system. In: *Proceedings of ICME international conference on complex medical engineering (CME)*, Beijing, China, 25–28 May 2013, pp.302–306. New York: IEEE.
26. Frisoli A, Loconsole C, Leonardis D, et al. A new gaze-BCI-driven control of an upper limb exoskeleton for rehabilitation in real-world tasks. *IEEE T Syst Man Cy C* 2012; 42: 1169–1179.
27. Kim H, Miller LM, Fedulow I, et al. Kinematic data analysis for post-stroke patients following bilateral versus unilateral rehabilitation with an upper limb wearable robotic system. *IEEE T Neur Sys Reh* 2013; 21: 153–164.
28. Ren Y, Kang SH, Park HS, et al. Developing a multi-joint upper limb exoskeleton robot for diagnosis, therapy, and outcome evaluation in neurorehabilitation. *IEEE T Neur Sys Reh* 2013; 21: 490–499.
29. Hsu LC, Wang WW, Lee GD, et al. A gravity compensation-based upper limb rehabilitation robot. In: *Proceedings of American control conference (ACC)*, Montreal, QC, 27–28 June 2012, pp.4819–4824. New York: IEEE.
30. DIAGNOBOT video. <https://www.youtube.com/watch?v=UsHrFRsW-Fo> (accessed 5 October 2017).
31. Swevers J, Ganseman C, Schutter JD, et al. Experimental robot identification using optimised periodic trajectories. *Mech Syst Signal Pr* 1996; 10: 561–577.
32. Hogan N. Impedance control: an approach to manipulation. In: *Proceedings of American control conference*, San Diego, CA, 6–8 June 1984, pp.304–313. New York: IEEE.
33. Hogan N. Impedance control: an approach to manipulation: part II. *J Dyn Syst: T ASME* 1985; 107: 8–16.